Epidermal Deletion of HIF-2α Stimulates Wound Closure

Andrew S. Cowburn[1,2], Laura E. Crotty Alexander[3], Mark Southwood[1], Victor Nizet[4], Edwin R. Chilvers[1] and Randall S. Johnson[2]

Wound closure requires a complex series of micro-environmentally influenced events. A key aspect of wound closure is the migration of keratinocytes across the open wound. It has been found previously that the response to hypoxia via the HIF-1α transcription factor is a key feature of wound closure. The need for hypoxic response is likely due to interrupted wound vasculature, as well as infection, and in this work we investigated the need for a highly related hypoxic response transcription factor, HIF-2α. This factor was deleted tissue specifically in mice, and the resulting mice were found to have an accelerated rate of wound closure. This is correlated with a reduced bacterial load and inflammatory response in these mice. This indicates that manipulating or reducing the HIF-2α response in keratinocytes could be a useful means to accelerate wound healing and tissue repair.

Journal of Investigative Dermatology (2014) **134,** 801–808; doi:10.1038/jid.2013.395; published online 31 October 2013

INTRODUCTION

Many processes supporting oxygen homeostasis are mediated by a small group of transcriptionally active hypoxia-inducible factors (HIFs). These transcription factors are considered to be the major coordinators of the cellular and systemic responses to hypoxia. HIF is a heterodimer composed of an oxygen-regulated HIF-α subunit (HIF-1α, HIF-2α, or HIF-3α) and the ubiquitous aryl hydrocarbon receptor nuclear translocator (HIF-1β). Under normoxic conditions, HIF-α protein turnover is generally very rapid because of the action of a set of prolyl hydroxylases; these oxygen-dependent enzymes hydroxylate two proline residues on the HIF-α subunit (Pro402 and Pro564), which promotes binding of the Von Hippel–Lindau (VHL) protein and subsequent targeting of HIF-α for poly-ubiquitination and proteasomal degradation. Despite its close proximity to an oxygen-rich ambient environment, the skin is well recognized to be constitutively hypoxic even under normal conditions (Stewart *et al.*, 1982; Varghese *et al.*, 1986; Bedogni *et al.*, 2005), resulting in a degree of constitutive HIF-1α stability in the basal epidermal layer.

In recent years, the importance of HIF-1α in wound healing has gained notoriety, with a number of groups demonstrating the role of this transcription factor in the cascade of events leading to wound closure. Following acute injury, the wound area becomes increasingly hypoxic owing to the loss of vascular structure and the heightened oxygen consumption accompanying the inflammatory response (Varghese *et al.*, 1986). This hypoxic micro-environment further enhances HIF-1α stability and promotes the release of a number of angiogenic factors (vascular endothelial growth factor, fibroblast growth factor-2, phosphatidylinositol glycan anchor biosynthesis, and angiopoietin 2)(Asahara *et al.*, 1999; Rehman *et al.*, 2003; Grunewald *et al.*, 2006; Yoder *et al.*, 2007) that regulate endothelial survival, migration, and proliferation, and the formation of new capillaries. Stabilization of dermal HIF-1α also increases the recruitment of circulating endothelial cell precursors to the wound site, which further improves wound revascularization and healing (Ceradini *et al.*, 2004; Jin *et al.*, 2006; Loh *et al.*, 2009). The role of HIF-1α in wound healing derives from a number of studies focused on the effects of depleting HIF-1α. Hence, in heterozygous HIF-1α knockout mice, the recruitment of endothelial cells is impaired and wound closure is delayed (Zhang *et al.*, 2010).

Reduced levels of HIF-1α protein have been documented in a number of chronic conditions associated with impaired wound healing, including diabetes and aging (Botusan *et al.*, 2008; Loh *et al.*, 2009). HIF-1α enhances the mobility of keratinocytes and dermal fibroblasts through its influence on matrix metalloproteinase and integrin expression (Decline and Rousselle, 2001; Deonarine *et al.*, 2007). Furthermore, HIF-1α increases the expression of laminin-332 and subsequent interaction with its receptors integrin-α3β1 and α6β4,

[1]*Department of Medicine, University of Cambridge, Addenbrooke's Hospital, Cambridge, UK;* [2]*Department of Physiology, Development and Neuroscience, University of Cambridge, Cambridge, UK;* [3]*Pulmonary & Critical Care Section, VA San Diego Healthcare System, La Jolla, California, USA and* [4]*Division of Pediatric Pharmacology and Drug Discovery, UCSD School of Medicine, La Jolla, California, USA*

Correspondence: Randall S. Johnson, Department of Physiology, Development and Neuroscience, University of Cambridge, Downing Street, Cambridge CB2 3EG, UK. E-mail: rsj33@cam.ac.uk

This work was conducted in both: Division of Biological Sciences, University of California, San Diego, La Jolla, California, USA, and Department of Physiology, Development and Neuroscience, University of Cambridge, Cambridgeshire, UK.

Abbreviations: CFU, colony-forming units; MPO, myeloperoxidase; Myc, myelocytomatosis; NOS, nitric oxide synthase; VHL, Von Hippel–Lindau; WT, wild-type

Received 3 June 2013; revised 28 August 2013; accepted 28 August 2013; accepted article preview online 13 September 2013; published online 31 October 2013

activating a signaling cascade to promote cell proliferation, survival, and migration (Decline and Rousselle, 2001; Iyer *et al.*, 2005; Deonarine *et al.*, 2007; Fitsialos *et al.*, 2008; Keely *et al.*, 2009).

In contrast, a potential role for HIF-2α in wound closure remains undefined. Although the two HIFα isoforms share a highly conserved amino acid sequence and structure, and are both stabilized under hypoxia and purported to bind the same HRE site, these isoforms appear to have distinct physiological roles. A differential function of HIF-1α and HIF-2α is supported by studies showing non-concordant expression and stability of these isoforms within different cell types and tissues. For example, HIF-1α is stabilized for sustained periods in the brain even after moderate hypoxia, compared with the liver and kidney, where HIF-1α stabilization requires more severe oxygen depletion, and is only transient (Stroka *et al.*, 2001). In contrast, HIF-2α is stabilized very readily in the liver, but only weakly in the kidney and the brain, and its expression tends to be maintained for much longer time periods (Wiesener *et al.*, 2003). These observations show clear differences between HIF-1α and HIF-2α, as supported by evidence indicating that HIF-1α and HIF-2α can act in a divergent manner to regulate a range of responses *in vivo*. Such counter-regulatory roles include functionally opposing interactions with the myelocytomatosis (Myc) transcription factors (Gordan *et al.*, 2007; Florczyk *et al.*, 2011) and with the tumor suppressors p53 (Bertout *et al.*, 2009) and mTOR (Toschi *et al.*, 2008). In addition, we have shown that nitric oxide homeostasis in macrophages can be differentially regulated through the opposing actions of T-cell helper-1 and T-cell helper-2 cytokines on the transcription of HIF-1α and HIF-2α (Takeda *et al.*, 2010).

To address whether the differential expression of HIF-1/2α isoforms in keratinocytes might affect the physiological process of wound closure, we have used a murine model of HIF-2α knockout targeted to keratinocytes (K14cre-HIF-2α animals). These mice have normal HIF-1α expression and normal dermal structure, but demonstrate accelerated wound closure. We have also used a different murine model to heightened HIF-1α stability, the K14cre-VHL/HIF-2α mouse, where deletion of both VHL and HIF-2α from keratinocytes leaves the HIF-1α isoform constitutively stable. This model again results in substantially accelerated wound closure, which is most evident during the initial healing phase.

RESULTS

Keratinocyte migration is accelerated by hypoxia

The migration of human keratinocytes is a critical factor underlying efficient and rapid wound healing. Previous studies have reported the ability of hypoxia to stabilize HIF-1α in the human keratinocyte cell line HaCaT (Fitsialos *et al.*, 2008) and the expression of HIF-1α at the leading edge of the wound margin in murine models. The HIF-1α target laminin-332 and its interaction with integrins α3β1 and α6β4 has also been linked to increased keratinocyte migration (Fitsialos *et al.*, 2008). In our initial experiments, we confirmed the influence of hypoxia on keratinocyte migration. HaCaT cells cultured under hypoxia (1% O_2) for 16 hours resulted in a significant increase in keratinocyte mobility compared with normoxic culture conditions (21% O_2) (Figure 1a). We were also able to show that HaCaT cells express HIF-2α in addition to HIF-1α and that they have the ability of hypoxia to enhance HIF-2α stability (Figure 1b).

Inflammatory responses during wound closure

The sequence of cellular events that follows experimental skin wounding is well documented. Several studies have documented the time course of the ensuing inflammatory cell infiltrate and the subsequent expression of antimicrobial

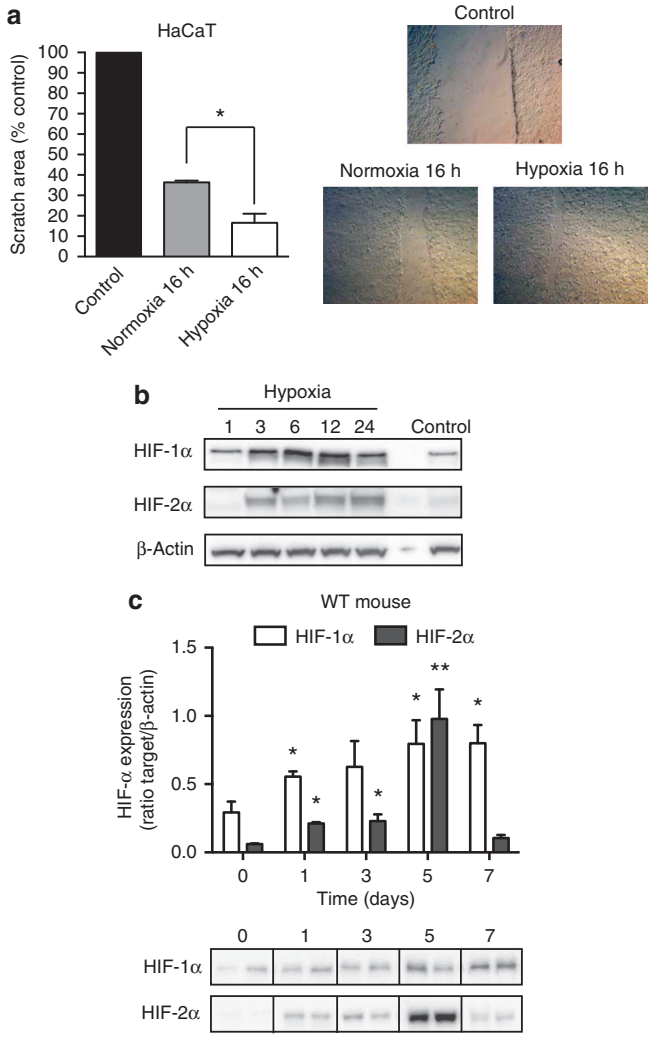

Figure 1. Hypoxia increases the speed of migrating keratinocytes. HaCaT cells were grown to 85% confluence before undertaking a scratch assay under normoxic (21%) and hypoxic (1% oxygen) conditions. (**a**) The scratch area was calculated from a digital image taken initially and 16 hours post culture. Data shown as the scratch area as a percentage of control ($n=8$, $^*P<0.05$). Photomicrographs show representative keratinocyte migration speeds. (**b**) Representative western blot showing the stability of HIF-1α and HIF-2α in the keratinocyte cell line HaCaT after exposure to hypoxia (1% oxygen). Cells were harvested at 0, 1, 3, 6, 12, and 24 hours post hypoxia. (**c**) Wounds from wild-type (WT) mice ($n=4$) were harvested at days 1, 3, 5, and 7, lysed, and western blotted for HIF-1α and HIF-2α protein stability. The bar graph shows the ratio of HIF-α against β-actin (au ± SEM) control with a representative western blot below.

peptides, nitric oxide synthase 1–3 (NOS1–3) and arginase-1/-2 in the wound margin during the closure period. We wished to confirm these findings in wild-type (WT) mice and compare them with changes observed in the K14cre-HIF-2α mouse. We performed 8 mm circular full-thickness punch biopsies on the back skin of 10–12-week-old WT mice; wounds were harvested at days 1–13. Bacterial counts (colony-forming units (CFU)) within the wound margin, including members of the normal skin microflora, were assessed by dilution plating on Todd–Hewitt broth agar plates. Bacterial colonization of the wound area was observed during the acute inflammatory phase (days 1–3), and thereafter the number of CFU diminished until day 5 when the wound area exhibited a full sanguineous crust (Figure 2a). This crust forms a protective barrier that is subsequently recolonized in association with a second CFU peak at day 10. The crust then recedes, paralleled with a reduction in the CFU counts, with normal flora colonization restored by day 13.

Inflammatory cell infiltration into the wound area was determined by using specific qPCR primers for myeloperoxidase (MPO) and F4/80 (Figure 2b) antimicrobial cathelicidin, CRAMP (Figure 2c), NOS1–3 (Figure 2d), and arginase-1/-2 expression (Figure 2e). These data confirm previous observations of an initial rapid inflammatory cell infiltration on days 1–3, followed by a prolonged, lower-magnitude macrophage response (days 1–7). The expression of CRAMP parallels very closely the MPO signal, suggesting that it may be principally neutrophil derived. NOS-2 also increased rapidly in the open wound, and then slowly decreased as the wounds closed, returning to near-normal expression by day 13; by contrast, NOS-1 and NOS-3 expression was relatively stable throughout the closure period. Arginase-1 and -2 were increased in the wound margin from days 2 to 9, possibly reflecting their role in collagen deposition.

HIF-α stability in the wound margin during closure

It is well established that mouse skin is hypoxic even under physiological conditions, and previous groups have shown HIF-1α stability at the wound margin. Consequently, we determined the stability profile for both HIFα isoforms during the initial 7-day period post wounding. Full-thickness dermal wounds were harvested from four WT mice at days 1, 3, 5, and 7 post wounding, and the expression of HIFα isoforms was determined by western blotting. As anticipated, HIF-1α expression increased over the closure period before plateauing at days 5 and 7. We also demonstrated an increase in HIF-2α stability on days 1, 3, and 7, with a significant increase in expression by day 5 (Figure 1c). Previous studies have also documented the expression profiles of HIF-α target genes arginase-1/-2 and NOS2 over the wound closure period. We further analyzed the wound samples (Supplementary Figure 1 online) and showed enhanced expression of both arginase-2 and NOS2 across the wound closure time course with little change in NOS3 expression.

Wound closure is accelerated in the K14cre-HIF-2α mice

To address the *in vivo* role of HIF-2α in the physiology of wound closure, we next generated mice in which HIF-2α deficiency was restricted to keratinocytes by crossing mice homozygous for the floxed HIF-2α allele with mice expressing Cre recombinase under the control of the keratinocyte promoter (K14cre). Adult K14cre-HIF-2α and WT male mice (10–12 weeks old) received an 8-mm full-thickness dermal punch biopsy on the back. Wound closure was measured digitally over the next 10 days. We found wound closure speed to be significantly increased in the K14cre-HIF-2α mice compared with age-matched WT mice ($n=12$); this was most evident at days 3–6, with the wound closure speed converging to match the normal WT by day 7 (Figure 3a) ($n=15$). Analysis of keratinocyte migration at the wound margin was determined by calculating the leading edge ratio, i.e., the distance covered by the keratinocyte leading edge divided by the overall wound margin. This ratio was significantly greater in the K14cre-HIF-2α mice ($n=6$) when compared with WT control ($n=6$) (Figure 3b and c). High-magnification photomicrographs of H&E-stained wound margins from WT and K14cre-HIF2α mice showed significantly greater keratinocyte motility in the HIF-2α mutants (Figure 3d). The enhanced keratinocyte motility may be linked to altered expression/activity of c-Myc and its overall influence of cell cycle progression. Given that a number of recent publications have described the opposing roles of HIF-1α and HIF-2α on c-Myc activity, we proceeded to analyze the expression of a number of c-Myc targets (Supplementary Figure 2 online). Keratinocyte deletion of HIF-2α significantly reduced the expression of CDKN1a and influenced a reduction in CDKN1b and E2F1 expression when compared with WT control.

Reduced acute inflammatory responses in K14cre-HIF-2α mice

Having previously described the importance of keratinocyte HIF-1α in the transcriptional regulation of two antimicrobial factors, cathelicidin and nitric oxide, we proceeded to analyze the wounds from the K14cre-HIF-2α mice for bacterial counts (CFU) during the initial inflammatory phase (days 1–3) (Figure 4a). Curiously, deletion of epidermal HIF-2α lowered recovered CFU by at least 1-log order on days 1 and 2 when compared with WT control mice (Figure 4a). Furthermore, qPCR analysis for MPO expression in the wound margin was also significantly lower in K14cre-HIF-2α mice on day 2 (Figure 4b), consistent with reduced neutrophil recruitment and inflammatory response. The expression profile for CRAMP (Figure 4c) matched that for MPO, with a significant reduction in the HIF-2α mutant mice. However, little change was noted in the expression for NOS1—3 (Figure 4d) between K14cre-HIF-2α mice and WT controls.

Epidermal deletion of VHL and HIF-2α increases wound closure

As a key regulator of HIFα protein stability, the effects of deleting the tumor suppressor VHL were examined in combination with HIF-2α deletion, by generating a K14cre-VHL/HIF-2α mouse. As anticipated, the resultant increase in keratinocyte HIF-1α expression (Supplementary Figure 3 online) in these mice greatly increased wound closure between days 1 and 5 (Figure 5a). The exaggerated wound closure is depicted in the photomicrographs taken from WT versus K14cre-VHL/HIF2α mice between days 1 and 9

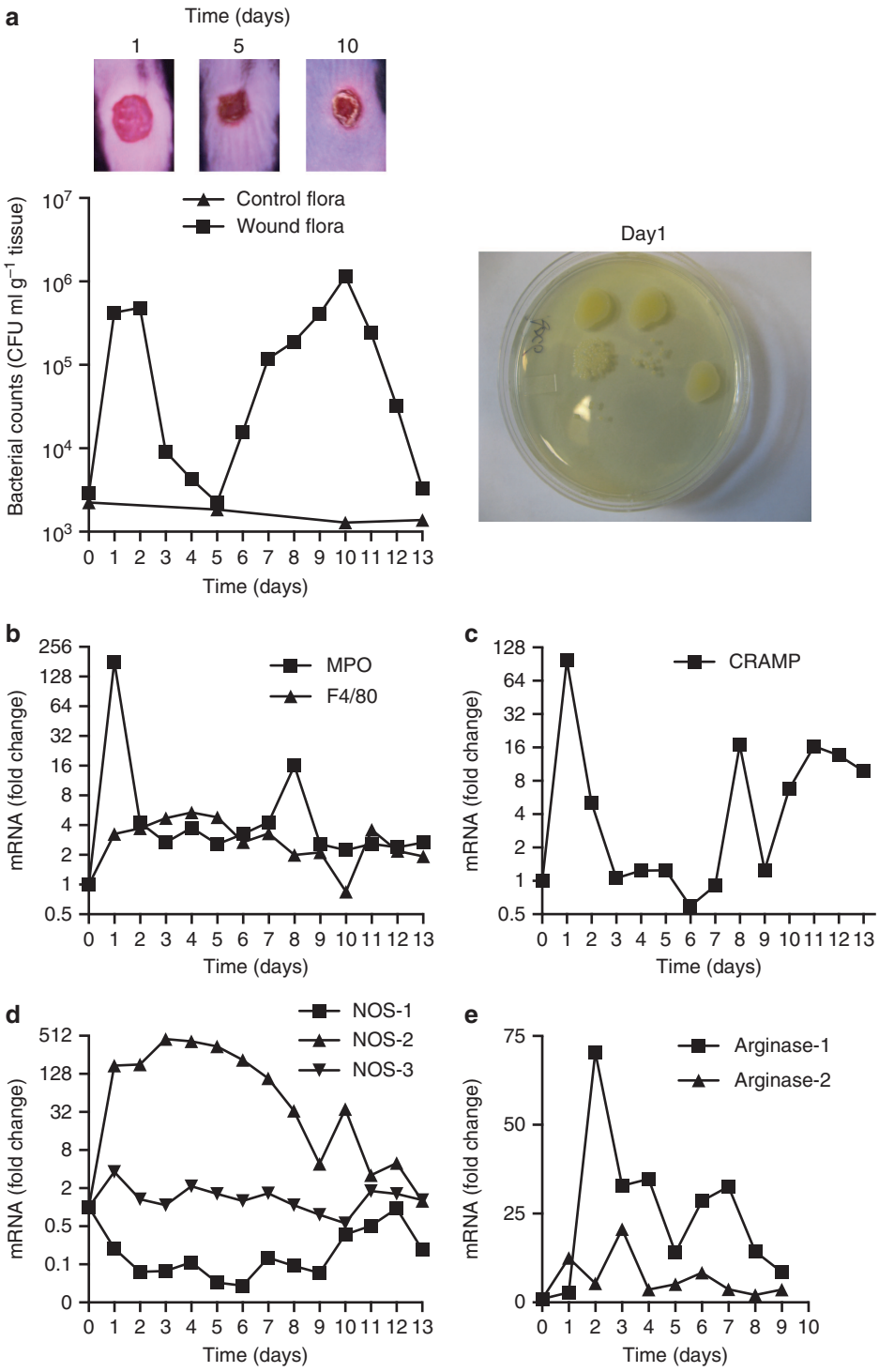

Figure 2. Characterization of environmental bacterial flora and inflammatory response genes during wound closure. (**a**) Wounds were harvested from wild-type mice throughout the closure period and bacterial flora (CFU mg^{-1} protein) was determined. Photomicrographs above the graphic show the general state of the wounds at the time in days shown. Photomicrograph to the right of the graphic shows a representative bacterial culture plate at day 1. (**b**, **c**, **d**, and **e**) QPCR analysis (fold change) of primers for MPO, F4/80, CRAMP, NOS1-3, and arginase-1 and 2 from wild-type wounds during the experimental period. CFU, colony-forming units.

(Figure 5b). Detailed analysis of wound samples during the initial 3 days (acute inflammatory phase) showed bacterial counts to be significantly lower on days 1 and 2 post wounding.

The marginal increase in CRAMP and MPO expression in the K14cre-VHL/HIF-2α mice at baseline could partly account for the lower initial bacterial counts. Fewer bacteria would be predicted to result in a reduced acute inflammatory response,

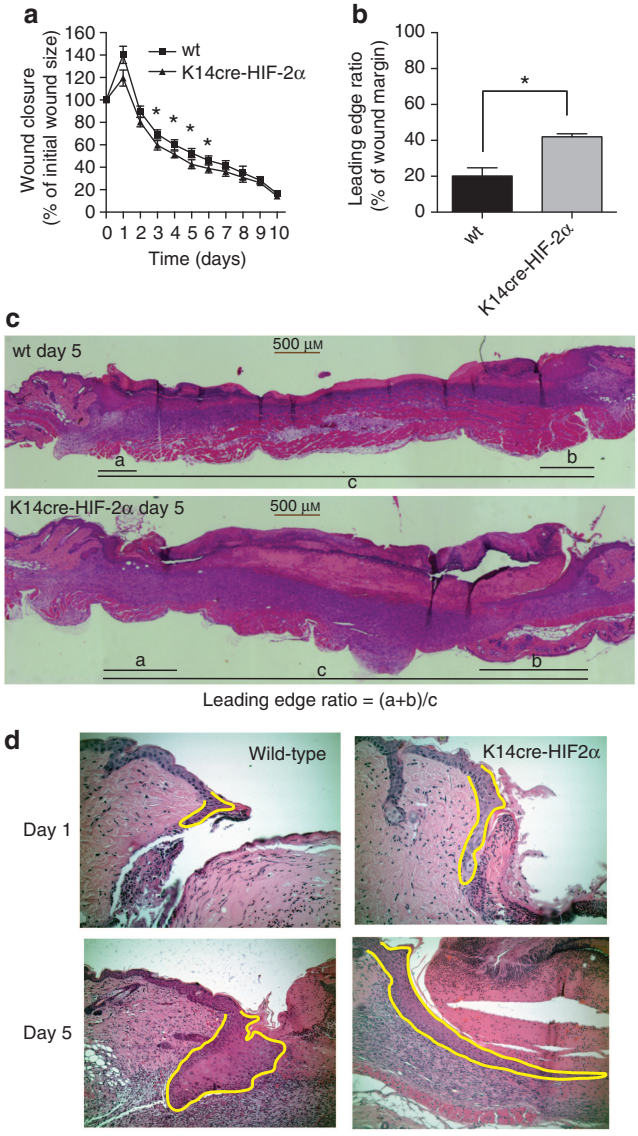

Figure 3. K14cre-HIF-2α mice show a faster wound closure and keratinocyte migration speed. (**a**) Digital images of wounds from K14cre-HIF-2α ($n=12$) and wild-type (wt) ($n=15$) mice were analyzed daily throughout the closure period. The data are presented as percentage wound closure compared with the original wound size (*$P<0.05$). (**b** and **c**) Keratinocyte leading edge analysis. Digital images of H&E-stained wounds were captured using a Leica scope and software. The distance of keratinocyte migration divided by the total distance of the wound margin gave a leading edge ratio (leading edge ratio = (a + b)/c). The keratinocyte leading edge from the K14cre-HIF-2α wound margin ($n=6$) was significantly greater than in the wild-type controls ($n=6$) (*$P<0.05$). (**d**) High magnification of H&E-stained wounds from wild-type and K14cre-HIF-2α mice taken on days 1 and 5. Yellow lines outline the migrating keratinocyte leading edge.

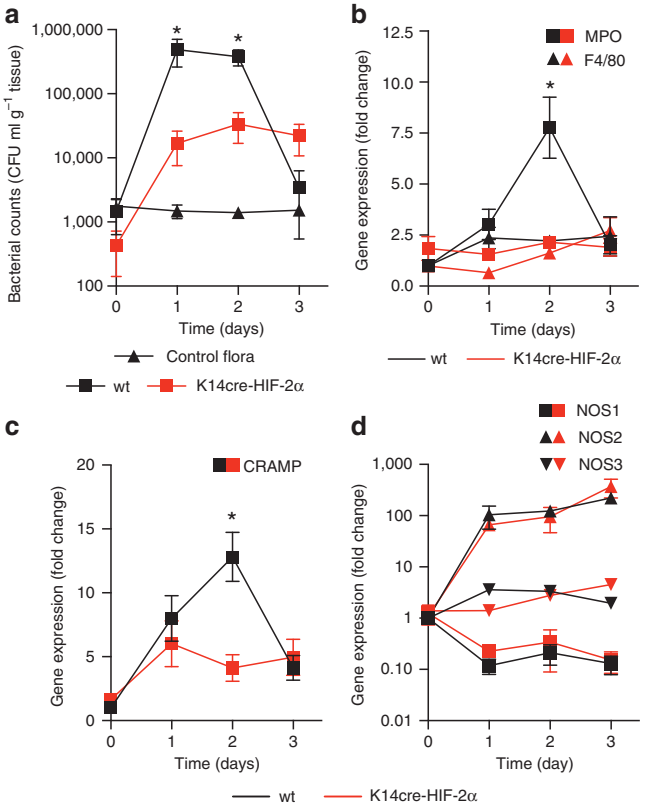

Figure 4. K14cre-HIF-2α mice show reduced wound environmental bacterial flora and reduced acute inflammatory responses. (**a**) Bacterial flora (CFU per mg tissue) were calculated from the wounds of K14cre-HIF-2α ($n=4$) and wild-type control ($n=4$) during the initial 3 days post wounding, and compared with normal background bacterial flora (control). (**b** and **c**) QPCR analysis (fold change) of primers for MPO, F4/80, and CRAMP showed a significantly reduced signal in the wounds from K14cre-HIF-2α ($n=4$) mice on day 2 when compared with wild-type control ($n=4$). (**d**) QPCR analysis (fold change) of NOS1–3 showed little deviation between K14cre-HIF-2α ($n=4$) and wild-type controls ($n=4$). CFU, colony-forming units; wt, wild type.

perhaps reflected in a lower MPO and CRAMP response on day 1 post wounding compared with WT controls. Although we suggest that the acute inflammatory response in the open wound is potentially lower in the K14cre-VHL/HIF-2α mice, the expression of NOS1 and NOS3 in the mutant mice were not different from WT controls, and NOS2 trended toward a higher expression on days 2 and 3 post wounding.

DISCUSSION

There is a great deal of experimental evidence suggesting that the initial heightened hypoxic environment within an open wound is pivotal in promoting tissue repair, in part through increasing the stability of HIF-1α (Tandara and Mustoe, 2004). The purpose of this study was to assess for the first time the involvement of HIF-2α in wound closure using an *in vivo* conditional keratinocyte knockout model. The results of this study show that HIF-2α is stabilized in the wound margin from day 1 to day 7, and that K14cre-HIF-2α mice lacking keratinocyte HIF-2α expression show the following: (i) significantly increased wound closure speed at early time points, (ii) increased keratinocyte migration at the leading edge of the wound, and (iii) reduced bacterial load in the open wound during the initial acute inflammatory phase. These striking effects of keratinocyte HIF-2α deletion were accentuated when VHL was coordinately deleted (Figure 5). This manuscript therefore reveals opposing roles for keratinocyte HIF-2α when compared with the established role of HIF-1α in wound healing.

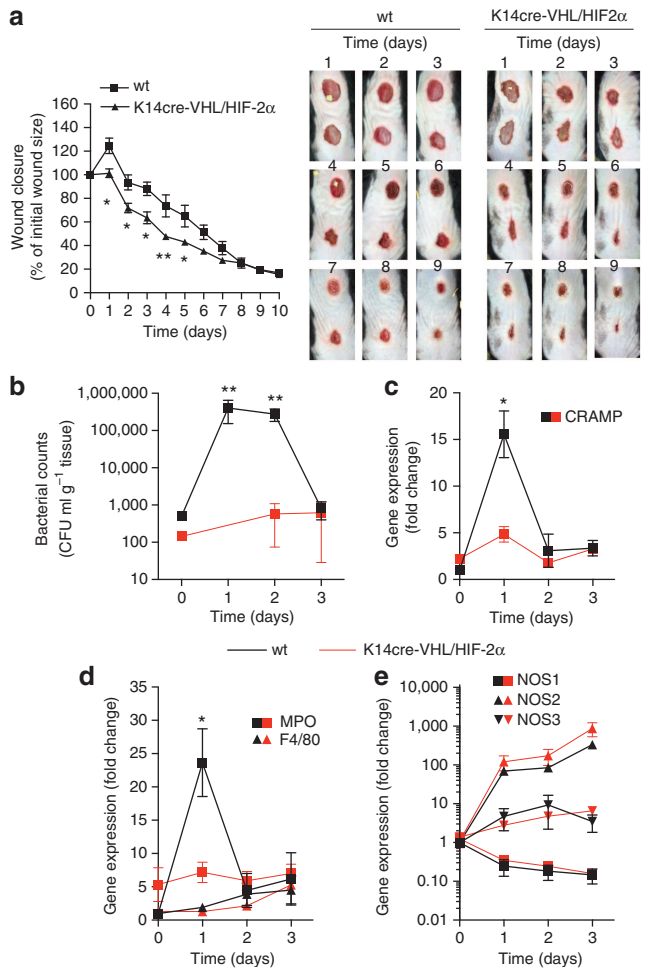

Figure 5. K14cre-VHL/HIF-2α mice show faster wound closure between days 1 and 5. (**a**) Digital images of wounds from K14cre-VHL/HIF-2α ($n=8$) and wild-type ($n=12$) mice were analyzed daily throughout the closure period. The data are presented as percentage wound closure compared with the original wound size (*$P<0.05$). Digital photomicrographs show representative images of wound closure from days 1 to 9 for wild-type and K14cre-VHL/HIF-2α mice. (**b**) Bacterial flora (CFU per mg tissue) was calculated from the wounds of K14cre-VHL/HIF-2α ($n=3$) and wild-type control ($n=4$) during the initial 3 days post wounding. (**c** and **d**) QPCR analysis (fold change) of primers for CRAMP and MPO, F4/80 showed a significantly reduced signal in the wounds from K14cre-VHL/HIF-2α ($n=3$) on day 1 when compared with wild-type control ($n=4$). (**e**) QPCR analysis (fold change) of NOS1-3 showed little deviation between K14cre-VHL/HIF-2α ($n=3$) and wild-type controls ($n=4$).

The contrasting roles of HIF-1α and HIF-2α become all the more pertinent when consideration is given to the interactions of HIF-α with Myc transcription factors (Gordan *et al.*, 2007). HIF-2α is known to augment c-Myc activity through the stabilization of c-Myc:Max complex, which promotes cell cycle progression; in contrast, HIF-1α inhibits the function of c-Myc, resulting in cell cycle arrest. Hence, Waikel and colleagues (Waikel *et al.*, 2001) have shown that targeted overexpression of c-Myc in epidermal stem cells (K14) results in the loss of hair follicles and the spontaneous development of ulcerated lesions due to severely impaired wound closure. Their model demonstrated a severe depletion in the number of epidermal stem cells and a significant impairment of keratinocyte migration. Therefore, in our keratinocyte model, deleting HIF-2α will enable HIF-1α to function unopposed, thus reducing the activity of c-Myc and subsequently increasing keratinocyte migration at the leading edge.

Previously, we have shown a central role for HIF-1α in the production of cathelilcidin antimicrobial peptides within the epidermis. In the normal or physiologically hypoxic environment of the skin, epidermal deletion of HIF-1α markedly increased the susceptibility of the skin to infection with group-A Streptococcus (Peyssonnaux *et al.*, 2008). In addition, pharmacological stabilization of HIF-1α limits *Streptococcus aureus* proliferation and lesion formation in a mouse skin abscess model (Okumura *et al.*, 2012). The majority of dermal wounds are colonized with aerobic and anaerobic bacteria, and the density and type of these bacteria are important in predicting wound closure speed (Bowler *et al.*, 2001). The mice for this study were individually housed in a clean facility to reduce cross-contamination and prevent the introduction of hostile pathogens. In this paper, we demonstrate reduced environmental bacterial counts on the skin of K14cre-HIF-2α mice, which remained significantly suppressed throughout the acute inflammatory phase of wound closure (days 1–3). This observation was further accentuated in the K14cre-VHL/HIF-2α mice, with environmental bacterial counts significantly lower across all time periods studied. Surgical aseptic practice aims to reduce bacterial load on the skin with the intent of lowering the intensity and duration of the inflammatory phase and to increase wound closure speed. The administration of prophylactic antibiotics has also been shown to significantly reduce postsurgical infections and increase wound closure speed.

In conclusion, our studies have shown a major role for HIF-2α in regulating wound healing and have highlighted the importance of individually determining the functional role of HIF-1α and HIF-2α in an *in vivo* physiological setting. We suggest that the epidermal deletion of K14cre-HIF-2α and the K14cre-VHL/HIF-2α is sufficient to increase the antimicrobial activity in the skin and reduce the acute inflammatory response, as shown by lower mRNA expression for MPO and CRAMP. These factors are likely to be reflected in the unopposed and beneficial effects of the hypoxia-HIF-1α-NOS2-nitric oxide pathway in wound repair. Our data predict that the development of a HIF-1α agonist or HIF-2α antagonist would provide a useful adjunct in a surgical setting to help boost the innate immune capacity of the skin and facilitate wound repair.

MATERIALS AND METHODS

K14cre-HIF-2α and K14cre-VHL/HIF-2α animals

All animals were housed in an approved facility, and experiments were conducted in accordance with the National Institute of Health guide for the care and use of laboratory animals. Targeted deletion of HIF-2α or VHL/HIF-2α in keratinocytes was created by crossing mice (C57Bl6/j) homozygous for the floxed allele in HIF-2α or VHL into a background of Cre recombinase expression driven by the K14 promoter, which is specific to cells of the keratinocyte lineage (Vasioukhin *et al.*, 1999; Boutin *et al.*, 2008). Deletion efficiency

and specificity for the K14cre was determined by comparing tissues from wt and K14cre-HIF1α mice for HIF1α expression. Of the tissues analyzed, only the skin showed a substantial reduction in HIF1α expression (Supplementary Figure 4 online). For wound healing assays, the hair on the back of the mice was shaved and depilated 24 hours before wounding to enable the normal bacterial flora to recover. Mice were anesthetized with 3% isoflurane and a single circular excisional wound of 8 mm diameter generated using a standard sterile biopsy punch that extended full thickness. The animals were caged individually and received buprenorphine at a dose of $100\,\mu g\,kg^{-1}$. For wound analysis, mice were euthanized and a standard area 2 mm beyond the original wound margin was excised. The wounds were dissected for histology, and analyzed for bacterial flora and specific mRNA and protein content. The tissues were either fixed in 4% PFA overnight or snap-frozen in liquid nitrogen and stored at $-80\,^{\circ}C$.

HaCaT scratch assay

HaCaT cells (supplied by CLS Cell Lines Service, Eppelheim, Germany), a spontaneously immortalized human keratinocyte line, were propagated in DMEM medium supplemented with 10% fetal calf serum. Cells were grown to 85% confluence and then transferred to an atmosphere of 1% or 21% O_2 for 12 hours before scratch injury by using a sterile 200-μl pipette tip. After injury, the medium was changed to remove cell debris. Digital images were taken from six wells and analyzed for wound closure speed using the Image J software (NIH, Bethesda, MD).

Morphological and immunohistochemistry analysis

Skin tissues were excised and fixed in 4% paraformaldehyde, embedded and sectioned in paraffin, and stained with hematoxylin and eosin (Sigma, Poole, UK). Digital images were taken on a Leica M165FC microscope using a Leica DFC310FX digital camera (Leica, Milton Keynes, UK). Images were analyzed using Image J software (NIH) and the leading edge equation adopted from Shirakata *et al.* (2005). HIF-1α IHC: formalin-fixed paraffin-wax-embedded skin biopsies were sectioned (4 μm) and incubated with monoclonal mouse anti-human HIF1α (1:100) (Novus Biologicals, Littleton, CO). Antibodies were detected using 3,3′-diaminobenzidine tetrahydrochloride to create a brown reaction product, counterstained with hematoxylin (Dako, Ely, UK), and examined by light microscopy.

RNA and DNA analysis

Total RNA was isolated from skin using TRI-reagent (Sigma), followed by RNA clean-up and DNase digest using RNeasy column kits (Qiagen, Manchester, UK). First-strand synthesis was performed with 1 μg of total RNA using a high-capacity cDNA kit (Applied Biosystems, Paisley, UK) according to the manufacturer's instructions. Relative gene expression was determined by qPCR (ABI Prism 7,700 sequence detection system, Applied Biosystems) and amplified in Sybr-green master mix (Applied Biosystems) using relevant primers from Qiagen. Relative gene expression levels were related to β-actin using the 2^{-CT} method (Livak and Schmittgen, 2001). DNA was isolated from tissues using TRI-reagent (Sigma). Taqman qPCR (ABI Step-one plus, Applied Biosystems) for HIF-1α (For 5′-ggtgctggtgt ccaaaatgtag Rev 5′-atgggtctagagagatagctccaca, probe 5′-FAMcctgtt ggttgcgcagcaag) was used to determine deletion efficiency by comparison with vascular endothelial growth factor expression (For 5′-tgaccatctgctttcgtgacc, Rev 5′-acttgttgcaggcagcgg, probe 5′-FAMtgct ccctgggctcgacagg). A concentration of $10\,ng\,\mu l^{-1}$ DNA was used per reaction with Taqman universal reaction master mix (Roche, Nutley, NJ).

Immunoblotting

Tissue samples were lysed in radio immunoprecipitation assay buffer. A total of 50 μg of whole-cell lysate was loaded onto a 4–12% Tris-acetate gel from Invitrogen (Paisley, UK) (NuPAGE). Immunoblotting analysis was performed using standard methods. The primary antibodies used in this study were as follows: rabbit polyclonals to anti-HIF-1α, anti-HIF-2α (1:1,000 Novus Biologicals, Cambridge, UK), anti-NOS2, anti-NOS3, and anti-arginase-II (1:200, Santa Cruz Biotechnology, Dallas, TX). The secondary antibody used was goat anti-rabbit IgG-HRP (1:2,000 RnD Systems, Abingdon, UK).

Statistic analysis

All data represent the mean (±SEM) of (*n*) separate experiments unless otherwise stated. Differences between groups were assessed using the *t*-test unless otherwise stated. A *P*-value <0.05 was considered significant.

CONFLICT OF INTEREST

The authors state no conflict of interest.

ACKNOWLEDGMENTS

This work was funded by Cambridge NIHR BRC, Papworth Hospital NHS trust, The Wellcome Trust (WT092738MA), and the National Institutes of Health (5R01AI093451).

SUPPLEMENTARY MATERIAL

Supplementary material is linked to the online version of the paper at http://www.nature.com/jid

REFERENCES

Asahara T, Takahashi T, Masuda H *et al.* (1999) VEGF contributes to postnatal neovascularization by mobilizing bone marrow-derived endothelial progenitor cells. *The EMBO J* 18:3964–72

Bedogni B, Welford SM, Cassarino DS *et al.* (2005) The hypoxic microenvironment of the skin contributes to Akt-mediated melanocyte transformation. *Cancer Cell* 8:443–54

Bertout JA, Majmundar AJ, Gordan JD *et al.* (2009) HIF2alpha inhibition promotes p53 pathway activity, tumor cell death, and radiation responses. *Proc Ntl Acad Sci USA* 106:14391–6

Botusan IR, Sunkari VG, Savu O *et al.* (2008) Stabilization of HIF-1alpha is critical to improve wound healing in diabetic mice. *Proc Natl Acad Sci USA* 105:19426–31

Boutin AT, Weidemann A, Fu Z *et al.* (2008) Epidermal sensing of oxygen is essential for systemic hypoxic response. *Cell* 133:223–34

Bowler PG, Duerden BI, Armstrong DG (2001) Wound microbiology and associated approaches to wound management. *Clin Microbiol Rev* 14:244–69

Ceradini DJ, Kulkarni AR, Callaghan MJ *et al.* (2004) Progenitor cell trafficking is regulated by hypoxic gradients through HIF-1 induction of SDF-1. *Nat Med* 10:858–64

Decline F, Rousselle P (2001) Keratinocyte migration requires alpha2beta1 integrin-mediated interaction with the laminin 5 gamma2 chain. *J Cell Sci* 114:811–23

Deonarine K, Panelli MC, Stashower ME *et al.* (2007) Gene expression profiling of cutaneous wound healing. *J Translational Med* 5:11

Fitsialos G, Bourget I, Augier S *et al.* (2008) HIF1 transcription factor regulates laminin-332 expression and keratinocyte migration. *J Cell Sci* 121: 2992–3001

Florczyk U, Czauderna S, Stachurska A *et al.* (2011) Opposite effects of HIF-1alpha and HIF-2alpha on the regulation of IL-8 expression in endothelial cells. *Free Radic Biol Med* 51:1882–92

Gordan JD, Bertout JA, Hu CJ *et al.* (2007) HIF-2alpha promotes hypoxic cell proliferation by enhancing c-myc transcriptional activity. *Cancer Cell* 11:335–47

Grunewald M, Avraham I, Dor Y *et al.* (2006) VEGF-induced adult neovascularization: recruitment, retention, and role of accessory cells. *Cell* 124:175–89

Iyer V, Pumiglia K, DiPersio CM (2005) Alpha3beta1 integrin regulates MMP-9 mRNA stability in immortalized keratinocytes: a novel mechanism of integrin-mediated MMP gene expression. *J Cell Sci* 118:1185–95

Jin DK, Shido K, Kopp HG *et al.* (2006) Cytokine-mediated deployment of SDF-1 induces revascularization through recruitment of CXCR4+ hemangiocytes. *Nat Med* 12:557–67

Keely S, Glover LE, MacManus CF *et al.* (2009) Selective induction of integrin beta1 by hypoxia-inducible factor: implications for wound healing. *FASEB J* 23:1338–46

Livak KJ, Schmittgen TD (2001) Analysis of relative gene expression data using real-time quantitative PCR and the 2(-Delta Delta C(T)) Method. *Methods* 25:402–8

Loh SA, Chang EI, Galvez MG *et al.* (2009) SDF-1 alpha expression during wound healing in the aged is HIF dependent. *Plastic Reconstr Surg* 123:65S–75S

Okumura CY, Hollands A, Tran DN *et al.* (2012) A new pharmacological agent (AKB-4924) stabilizes hypoxia inducible factor-1 (HIF-1) and increases skin innate defenses against bacterial infection. *J Mol Med (Berl)* 90: 1079–89

Peyssonnaux C, Boutin AT, Zinkernagel AS *et al.* (2008) Critical role of HIF-1alpha in keratinocyte defense against bacterial infection. *J Invest Dermatol* 128:1964–8

Rehman J, Li J, Orschell CM *et al.* (2003) Peripheral blood "endothelial progenitor cells" are derived from monocyte/macrophages and secrete angiogenic growth factors. *Circulation* 107:1164–9

Shirakata Y, Kimura R, Nanba D *et al.* (2005) Heparin-binding EGF-like growth factor accelerates keratinocyte migration and skin wound healing. *J Cell Sci* 118:2363–70

Stewart FA, Denekamp J, Randhawa VS (1982) Skin sensitization by misonidazole: a demonstration of uniform mild hypoxia. *Br J Cancer* 45:869–77

Stroka DM, Burkhardt T, Desbaillets I *et al.* (2001) HIF-1 is expressed in normoxic tissue and displays an organ-specific regulation under systemic hypoxia. *FASEB J* 15:2445–53

Takeda N, O'Dea EL, Doedens A *et al.* (2010) Differential activation and antagonistic function of HIF-{alpha} isoforms in macrophages are essential for NO homeostasis. *Genes Dev* 24:491–501

Tandara AA, Mustoe TA (2004) Oxygen in wound healing–more than a nutrient. *World J Surg* 28:294–300

Toschi A, Lee E, Gadir N *et al.* (2008) Differential dependence of hypoxia-inducible factors 1 alpha and 2 alpha on mTORC1 and mTORC2. *J Biol Chem* 283:34495–9

Varghese MC, Balin AK, Carter DM *et al.* (1986) Local environment of chronic wounds under synthetic dressings. *Arch Dermatol* 122:52–7

Vasioukhin V, Degenstein L, Wise B *et al.* (1999) The magical touch: genome targeting in epidermal stem cells induced by tamoxifen application to mouse skin. *Proc Natl Acad Sci USA* 96:8551–6

Waikel RL, Kawachi Y, Waikel PA *et al.* (2001) Deregulated expression of c-Myc depletes epidermal stem cells. *Nature Genet* 28:165–8

Wiesener MS, Jurgensen JS, Rosenberger C *et al.* (2003) Widespread hypoxia-inducible expression of HIF-2alpha in distinct cell populations of different organs. *FASEB J* 17:271–3

Yoder MC, Mead LE, Prater D *et al.* (2007) Redefining endothelial progenitor cells via clonal analysis and hematopoietic stem/progenitor cell principals. *Blood* 109:1801–9

Zhang X, Liu L, Wei X *et al.* (2010) Impaired angiogenesis and mobilization of circulating angiogenic cells in HIF-1alpha heterozygous-null mice after burn wounding. *Wound Repair Regen* 18:193–201